

A critical review on soil ionisation modelling for grounding electrodes

MEHRDAD MOKHTARI¹, ZULKURNAIN ABDUL-MALEK², GEVORK B. GHAREHPETIAN¹

¹*Amirkabir University of Technology
Electrical Engineering Department
No. 424, Hafez Avenue, Tehran, Iran
e-mail: mokhtari1358@aut.ac.ir, grptian@aut.ac.ir*

²*Universiti Teknologi Malaysia
Institute of High Voltage and High Current (IVAT)
81310, Johor Bahru, Malaysia
e-mail: zulkurnain@utm.my*

(Received: 20.09.2015, revised: 27.11.2015)

Abstract: Grounding electrode resistance non-linearly changes under impulse conditions due to soil ionisation phenomenon. Several models have been proposed to model soil ionisation for grounding electrodes applications. However, to date, there is yet an attempt made to compile all these works into a comprehensive review article. Therefore, this paper is written with the objective of summarizing all related works in this field as a one-stop reference. With reference to the literature, this paper is written to summarize the working principles of the soil ionisation models as well as the accuracy and performance analysis of the models. This paper, particularly highlights the deficiencies of the available models in terms of accuracy and performance. This knowledge will contribute to the development of a new accurate and efficient soil ionisation model.

Key words: grounding electrodes, grounding electrode resistance, soil ionisation modelling

1. Introduction

Soil breakdown phenomenon occurs when the high impulse current discharges into the earth through the grounding conductors [1-5]. Due to the soil breakdown, the resistance of the soil and consequently the peak voltage response of the grounding electrode decrease. Therefore, the soil breakdown improves the efficiency of the grounding systems. Two main processes have been advanced to explain the increase of soil conduction during high impulse current discharges, namely, (1) thermal heating process and (2) soil ionisation process. In the thermal heating process, the discharged current increases the temperature of the existing water filling among the soil grains. Due to the heating process, the resistivity of the heated water

decreases, which in turn causes the resistivity of the bulk soil and consequently reduces the grounding electrode resistance [6-8]. In the soil ionisation process, the electric field enhancement in air voids enclosure among the soil grains, causing the soil breakdown occurrence [5, 9-11]. Since the resistance of the ionized air is much smaller than the resistance of the soil grains, the equivalent soil resistance decreases. It is noted that the soil ionisation is mostly accepted as the main factor in the soil breakdown phenomenon.

Several circuit models have been proposed to model the soil ionisation and its effect on the grounding electrode resistance. Despite the numerous published research studies carried out in this area, there appears to be an absence of a single, comprehensive review paper that provides evaluation on the advantages and drawbacks. With reference to the literature, this review paper is written with the following goals in mind: (1) to summarize the functions and working principles of the available soil ionisation models proposed by CIGRE [4], Bellaschi *et al.* [3], Nor *et al.* [12], and Liew and Darveniza [13], and (2) to evaluate the advantages and drawbacks of the mentioned soil ionisation models in terms of accuracy, complexity in the methodology used, and applications. At the end of the paper, a comparison among the soil ionisation models with respective experimental results is also provided. The remaining of the paper is organized as follows:

Section 2 presents the theoretical background to introduce the soil ionisation process and the characteristics of the grounding electrode resistance. In Section 3, the soil ionisation models are critically reviewed. Section 4 discusses the accuracy and the performance analysis of the soil ionisation models. Finally, the overall discussion and conclusions are given in Section 5.

2. Theoretical background

In this section, the soil ionisation process, as the most accepted process, is explained. Then, the key characteristics of the grounding electrode resistance under impulse current obtained from the experimental case are presented. These key characteristics have been used to investigate the accuracy and the performance of the proposed soil ionisation models by CIGRE [4], Bellaschi *et al.* [3], Nor *et al.* [12], and Liew and Darveniza [13].

2.1. Soil ionisation process

In a soil medium, the air voids and soil grains act as a mixed dielectric. This is because the conductivity and permittivity of the air voids (σ_{air} and ϵ_{air}) and soil grains (σ_{soil} and ϵ_{soil}) are different. Therefore, the displacement vectors at the interface between the air void and soil grain are equal, that is $E_{air}\epsilon_{air} = E_{soil}\epsilon_{soil}$. When current discharges into the earth, the resistive paths of the air void and soil grain act as a resistive voltage divider. Since the permittivity of the air is much greater than the permittivity of the soil grain, the electric field in the air void exceeds the breakdown level [14]. Due to the air breakdown, the ionized air forms arc inside the soil. In soil, the arc is fully developed at current peak. The volume at which the arc is conducting the current in the soil is called the arc channel. For the duration when current rises

from zero to peak, arc resistance is a function of current; by which increasing the current will reduce the arc resistance. The minimum value of the arc resistance is obtained at the current peak [13]. For the duration of the current in decay time, the resistance of the arc is mainly dependent on the energy balance between the arc channel and soil rather than current magnitude. By decreasing the energy stored in the arc channel, the resistance of the arc increases until the arc is extinguished in the soil. Soil dynamic resistance for any instance of time is obtained as equivalent parallel soil resistance and arc resistance. The soil dynamic resistance changes for the duration of impulse current since the resistance of the arc is changed. Due to the energy balance between the arc channel and soil, dynamic soil resistance would show a hysteresis characteristic [13, 15].

2.2. Grounding electrode resistance characteristics

In this section, an experimental case performed by Bellaschi *et al.* is discussed to explain the characteristics of the grounding electrode resistance. The experiment was set up using a driven 2.44-m-long electrode with a radius of 7.9 mm in soil with a resistivity value of 162 $\Omega\cdot\text{m}$ (Ground-M). The injected current had 6.6 kA-amplitude with 15 $\mu\text{s}/42 \mu\text{s}$ -waveform. The transient resistance through the experimental setup was obtained as an instantaneous ratio of voltage and current (Oscillogram CSH-2184-CH&CI).

Fig. 1 illustrates the current and voltage waveforms, as well as the variation of the grounding electrode resistance of the electrode. It is noted that the resistance was obtained as an instantaneous ratio of voltage and current, that is $R(t) = v(t)/i(t)$. As seen in this figure, the grounding electrode resistance value is nonlinearly changed when the impulse current is dispersed into the earth.

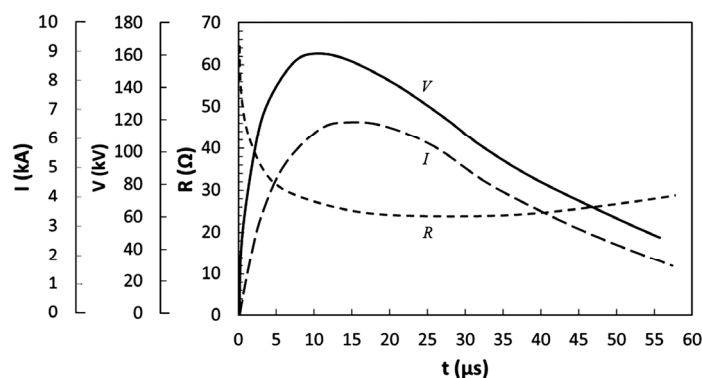


Fig. 1. Variation of grounding electrode resistance under impulse current discharge

For the duration when the current rises from zero to a peak value, the grounding electrode resistance is reduced from the measured low current ac value (64 Ω) to a more minimum value (24.5 Ω). The minimum value of the resistance is obtained around the current peak. For the duration when the current decreases from a peak value to zero, the grounding electrode resistance slowly increases in the measured low current ac value. This is because the energy stored in the arc channel does not allow the resistance to be quickly increased.

The slow increase of the resistance causes the hysteresis effect, as observed in the resistance-current characteristic presented in Fig. 2.

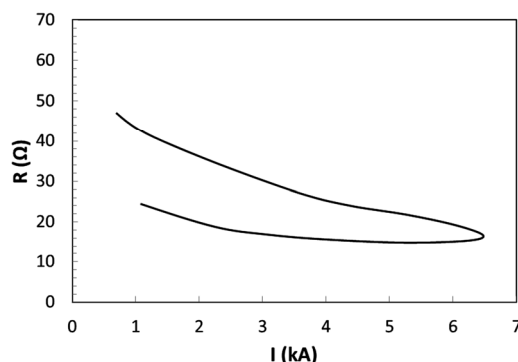


Fig. 2. Hysteresis characteristic of grounding electrode resistance

3. Soil ionisation models

In this section, the concept of the soil ionisation models suggested by CIGRE [4], Bellaschi *et al.* [3], Nor *et al.* [12], and Liew and Darveniza [13] is reviewed. In addition, the review highlights the advantages and drawbacks of the suggested models.

3.1. CIGRE model

The proposed model by CIGRE [4] is an empirical formula to compute the grounding electrode resistance as a function of current. In this model, the onset of the ionisation mainly depends on the soil resistivity. After soil ionisation onset, the grounding electrode resistance decreases with the logarithm of the current. CIGRE model considers the resistance of the ionized zone as zero. This model takes into account the equivalent geometry of the ionisation zone to compute the grounding electrode resistance, with consideration of soil ionisation. The simplified model considers computing the grounding electrode resistance under high amplitude currents to approach the square root dependence currents and low amplitude currents to approach the currents close to zero. In addition, the model approximates the logarithmic dependence between low and high amplitude currents. The suggested expressions to compute the grounding electrode resistance with soil ionisation consideration are

$$R_i = \frac{R}{\sqrt{1 + i(t)/I_g}}, \quad (1)$$

where R is the low current grounding electrode resistance in $[\Omega]$, and $i(t)$ is the impulse current in $[\text{kA}]$. I_g is the limit current in $[\text{kA}]$ at which the soil ionisation occurs and is given as

$$I_g = \frac{E_c \rho}{2\pi R^2}, \quad (2)$$

where ρ is the soil resistivity in [Ω .m] and E_c is the soil critical electric field intensity in [kV/m], which is recommended by CIGRE as 400 kV/m. However, a variety of E_c values had been suggested in many previous studies to apply in grounding electrode resistance computations, ranging from 50 kV/m [3] to 1500 kV/m [16]. As concluded in [17], the results obtained using CIGRE model and also the electromagnetic model are comparable when the correct values of E_c from [14] are taken into account. Therefore, it can be said that the accuracy of the CIGRE model to compute the grounding electrode resistance is dependent on E_c value. This model is simple and can be easily used in the circuit approaches. However, CIGRE model is only valid for the electrodes with maximum 30 m long [4]. This model does not consider the energy balance concept in the computations; therefore, this model cannot show the hysteresis characteristic of the grounding electrode resistance.

3.2. Bellaschi model

The proposed model by Bellaschi *et al.* [3] uses the basic formula for the computation of low current grounding electrode resistance value proposed by Dwight [18] formulas for single and multi-driven electrodes. For the single driven electrode, the following relation is taken into account

$$R = \frac{\rho}{2\pi l} \left[\ln \left(\frac{4l}{a} \right) - 1 \right], \quad (3)$$

where ρ is the soil resistivity in [Ω .m], l is the electrode length in [m], and a is the conductor radius in [m]. To consider the effect of soil ionisation in grounding electrode resistance, this model takes into account the geometry of the ionized zone as the new geometry of the grounding electrode. This is because the resistance of the arc is considered to zero. In this term, the length and the radius of the ionized zone are used as the conductor effective radius a_i and conductor effective length l_i . To compute the effective radius a_i , the following relation is taken into account.

$$a_i = \frac{ai(t)}{I_c}, \quad (4)$$

where a is the conductor radius in [m], $i(t)$ is the impulse current magnitude in [kA], and I_c is the critical current in [kA] at which the soil ionisation occurs at the surface of the electrode. To determine the critical current I_c , the following relation is used

$$I_c = \frac{2\pi a l E_c}{\rho}. \quad (5)$$

It is to be noted that E_c is obtained from the experiment setup of the grounding electrode, which needs to be modeled beforehand. The relation of a_i to the current is used to compute the conductor effective length l_i as

$$\frac{i(t)}{I_c} = \frac{a_i l_i}{al}. \quad (6)$$

This model can be used for the multi-electrode system. For this purpose, the effective radius and effective length are obtained from (4) to (6) with reference from the related formulas for computing the resistance of the multi-electrode system [18]. The Bellaschi model is simple and applicable to use in circuit approaches. However, the accuracy of the model is strongly dependent on E_c value. It is noted that this model does not consider the energy balance concept in the commutations.

3.3. Nor model

The proposed model by Nor *et al.* [12] is a circuit based model. The circuit includes series elements R_{rod} and L_{rod} to represent the resistance and inductance of the electrode, and two parallel branches consisting of R_1 - C_{sand} and R_2 - L circuits to represent the pre- and post-ionisation circuits, as shown in Fig. 3. The inductance L determines the required time delay for the ionisation. In the pre-ionisation branch, resistance R_1 represents the conduction of the soil due to thermal effect and soil properties with soil capacitive effect (C_{sand}). In the post-ionisation branch, R_2 resistance represents the conduction behavior after the ionisation is fully expanded. It should be noted that the value of the inductance L must be determined by trial and error. In addition, there is no relation proposed by Nor *et al.* to compute the value of C_{sand} .

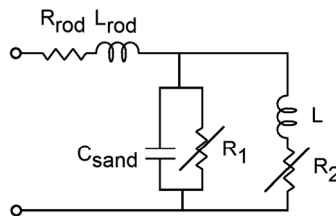


Fig. 3. Equivalent circuit model of soil ionisation proposed by Nor *et al.* [12]

The proposed model by Nor *et al.* is a general model that can be calibrated and applied to all types of impulse responses and soil samples. The aforementioned resistances R_1 and R_2 have a strong nonlinear voltage-current characteristic and need to be determined using the curve fitting method. However, it should be noted that the application of the curve fitting method may inherently cause error in determining the resistance value. The values of the resistances R_1 and R_2 as a function of the current are shown as $R_1(i)$ and $R_2(i)$. In this model, the ionisation time is taken into account. The dynamic soil resistance under impulse condition is expressed with

$$R(t) = R_1(i) \left(\frac{R_2(i)}{R_1(i)} + e^{t/\tau_i} \right), \quad (7)$$

where τ_i is the ionisation time constant. However, this model does not consider the deionisation time. The Nor model also cannot predict the resistance characteristics accurately for the

decay time duration of the impulse current. This model only adequately simulates the cases with pre- and post-ionisation characteristics. This model is simple, but suffers from the experimental data needed to obtain the resistances in the pre- and post-ionisation branches. The Nor model cannot accurately produce the correct grounding electrode resistance and its voltage response, unless the experimental data is used to calibrate the model. Finally, this model does not consider the energy balance concept because deionisation time is not considered in the model.

3.4. Liew-Darveniza model

The dynamic soil model proposed by Liew and Darveniza [13] takes into account the analytical relations to model the grounding electrode resistance with ionisation consideration. This model tries to describe the transient behavior of the soil at the instance of lightning strikes. The model considers the ionisation resistance of the ionized zone. In this model, three regions known as the ionisation region, deionisation region and non-ionisation region are introduced. However, this model cannot describe the arc phenomenon, which occurs in the vicinity of the driven rod, the area where the soil resistivity becomes zero. For this purpose, a modification of the model was later given in [19]. According to the modified model, the sparking region is considered as Region 4, as can be seen in Fig. 4. In this region, the current density of discharge current J is much higher than critical value J_c . In Region 3, the soil is ionized, and this ionisation is defused outward. The soil in Region 2 starts to recover because the current density J becomes lesser than critical value J_c . Finally, non-affected bulk soil is incorporated in the model as Region 1. The resistivity profile of the ionized soil as described is depicted in Fig. 5 to show the variation of the soil resistivity versus current density. At the instance of current discharge, the soil resistivity is ρ_0 and the soil is not ionized as seen in zone a. Upon the current density reaching the critical current density, J_c , the soil ionisation starts (zone b). At this moment, the soil resistivity is gradually reduced, as given in (8), and reaching the value of ρ .

$$\rho = \rho_0 \cdot e^{-\frac{t}{\tau_1}} \quad (8)$$

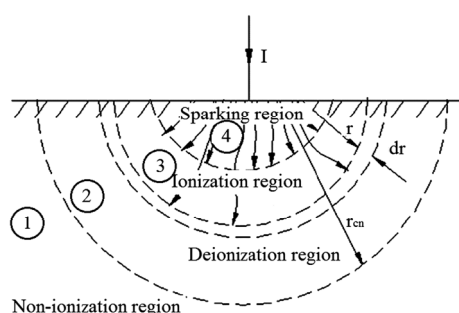


Fig. 4. Soil characteristics under impulse current in a hemispherical model for a direct sparking connection [19]

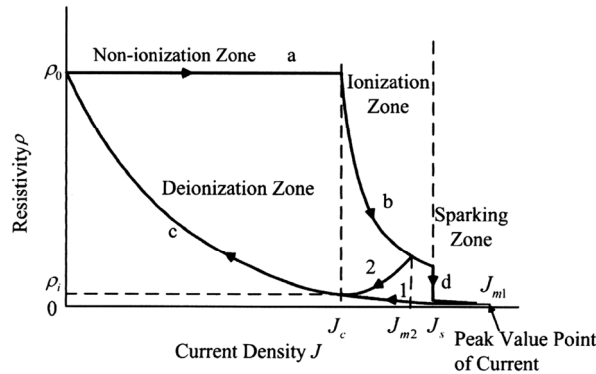


Fig. 5. The soil resistivity profile of the soil ionisation zone in Liew-Darveniza's model [13]

The ionisation time constant τ_1 is estimated as $2 \mu\text{s}$ and t is the time measured from the onset of the ionisation. If the current density exceeds the critical value, the tracking will puncture the soil (zone d). This current is shown by J_s as obtained by (9).

$$J_s = \alpha J_c \quad \text{and} \quad \alpha \geq 1, \quad (9)$$

where α is the coefficient, which is determined for any type of soil and has an exponential relation with current amplitude. If sparking does not occur, the soil recovers until the soil resistivity ρ recovers after τ_2 (zone c) according to (10).

$$\rho = \rho_i + (\rho_0 - \rho_i) \cdot (1 - e^{-t/\tau_2}) \cdot (1 - J/J_c)^2, \quad (10)$$

where ρ_i is the lowest value of the soil resistivity and the estimated time for recovery is $\tau_2 = 4.5 \mu\text{s}$.

Since $J_c = \rho E_c$, the correct value of the critical electric field E_c is essential to determine critical current density. Therefore, it can be said that the accuracy of the model strongly depends on the critical electric field value E_c , which is needed to obtain from the experimental setup. To compute the vertical grounding electrode resistance, the proposed formula by Liew and Darveniza is taken into account as

$$R = \frac{\rho}{2\pi l} \ln \frac{a+l}{a}. \quad (11)$$

However, the comparison between the computed resistances for different electrode length and radius obtained by Liew and Darveniza's formula and Dwight's formula shows about 10% difference [13]. Liew-Darveniza's model does not suitably explain the surge behavior of electrodes, in which high currents result in discrete-breakdown paths, rather than in a more diffused growth of increasing ionization [13]. Thus, more investigation is required to improve the model. An interpretation of the model by Sekioka *et al.* [20] reveals that Liew-Darveniza's model considers the energy balance concept. This model also shows the hysteresis characteristic of the grounding electrode resistance under impulse condition. In the equivalent circuit of the model, the electrode inductance and soil capacitance are neglected. This may cause

large errors in voltage response of the electrodes under fast and slow fronted currents when the inductive and capacitive characteristics become significant [21]. The methodology of the model, compared to the methodology of the other reviewed models, is more complex.

4. Accuracy analysis of the models

This section discusses the accuracy of the aforementioned models in terms of computing the grounding electrode resistance and voltage response. To show the accuracy of the models, the resistances and the voltage responses of the electrode models have been compared with the obtained results from the experiment [3]. For this purpose, the identified experimental case as Ground-F (Oscillogram CSH-2184-CO) from the well-known experimental study by Bellaschi *et al.* [3] is taken into account. The specifications of experimental case are presented in Table 1. It is noted that the critical electric field value is taken from [13] as 127 kV/m.

Table 1. The specifications of the grounding electrode from the experiment [3]

| Parameters | (GroundF) |
|--|-----------|
| Soil type | clay |
| Soil resistivity, ρ (Ω .m) | 80 |
| Electrode length, l (m) | 3.05 |
| Electrode radius, r (mm) | 12.7 |
| Current's amplitude, I_m (kA) | 11 |
| Current's T_f/T_h (μ s/ μ s) | 18/37 |
| Critical electric field, E_c (kV/m) [13] | 127 |

The grounding electrode resistance variations and the voltage responses obtained from the experiment (Ground-F) and obtained by the CIGRE, Bellaschi, Nor, and Liew-Darveniza's models are illustrated in Fig. 6. As seen in this figure, according to the experimental graph, the low current value of the grounding electrode resistance is 24.4 Ω at $t = 0$ and the minimum value of the grounding electrode resistance is obtained at $t = 20$ μ s at 10.9 Ω .

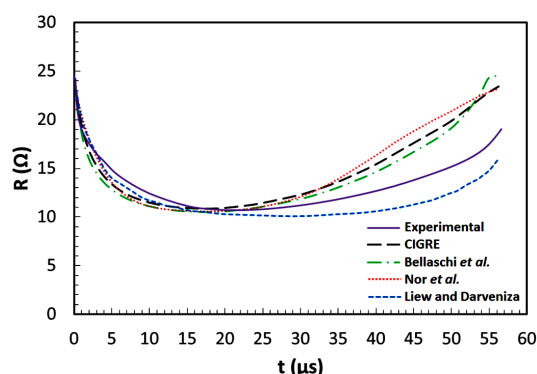


Fig. 6. The resistance variation of the grounding electrode

The values of the resistances computed by the models are presented in Table 2. According to Table 2, the accuracy of the models in terms of resistances computed for the low current and to satisfy minimum values is satisfactory compared to the experimental resistance values. However, it should be noted that only the Liew-Darveniza and Nor models compute the minimum resistance value around 20 μs , as observed in the experimental graph. However, the CIGRE and Bellaschi models compute the minimum value of the grounding electrode resistance at $t = 18 \mu\text{s}$. The resistance values obtained from the models for the time duration of $t = 0 - 18 \mu\text{s}$, compared to the experimental value, shows within 15% error. The error of the models to compute the grounding electrode resistance is increased after $t = 18 \mu\text{s}$. The maximum error is obtained at $t = 50 \mu\text{s}$ in 40%. In conclusion, according to Fig. 6, it can be stated that the error of the Liew-Darveniza's model in computing the grounding electrode resistance value among the models compared to the experimental resistance value is much lower.

Table 2. Grounding electrode resistance values obtained from the models and relevant errors compared to the experimental values

| Model | Low current resistance [Ω] | Error [%] | Minimum resistance [Ω] | Error [%] |
|----------------|-------------------------------------|-----------|---------------------------------|-----------|
| CIGRE | 24.5 | -0.4 | 10.8 | -0.9 |
| Bellaschi | 24.5 | -0.4 | 10.5 | -3.7 |
| Nor | 23.7 | -2.9 | 10.6 | -2.7 |
| Liew-Darveniza | 24.7 | 1.2 | 10.4 | -4.6 |

The hysteresis characteristics of the grounding electrode resistance computed by the models in comparison with the experimental value are illustrated in Fig. 7. CIGRE, Bellaschi, and Nor models fail to show the hysteresis characteristics of the resistance. It is because these models do not take into account the energy balance concept in their computations for the duration of current in decay time. In contrary, Liew-Darveniza's model shows the hysteresis characteristics of the resistance. However, the hysteresis characteristic shown by Liew-Darveniza's model has a difference compared to the one by the experiment.

The voltage waveforms of the electrodes computed by the models and obtained by the experiment are illustrated in Fig. 8. The peak value of the voltage according to the experiment is 120 kV.

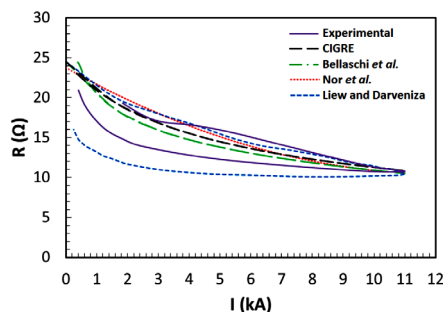


Fig. 7. The hysteresis characteristics of the grounding electrode resistance

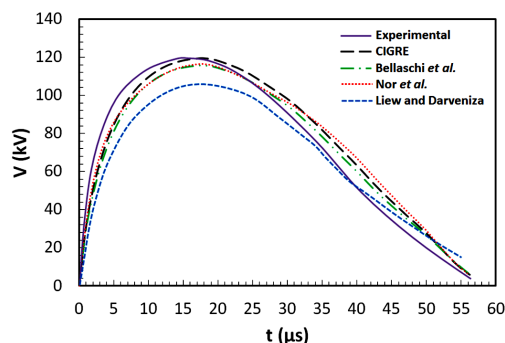


Fig. 8. The voltage response of the grounding electrode

The computed values by the models and their errors compared to the experimental value are presented in Table 3. The peak value of the voltage computed by the CIGRE and Nor model is close to the experimental value. On the contrary, Liew-Darveniza's and Bellaschi's models have errors in computing the voltage peak. The voltage waveforms of all models are different from the voltage waveform of the experiment. In addition, the peak values of the voltages computed by the models are lead lower compared to the experiment.

Table 3. The voltage peak values computed by the models and their errors compared to the experimental value (120 kV)

| Model | Voltage peak [kV] | Error [%] |
|----------------|-------------------|-----------|
| CIGRE | 118.9 | -0.9 |
| Bellaschi | 115.5 | -3.7 |
| Nor | 116.6 | -2.8 |
| Liew-Darveniza | 114.4 | -4.7 |

5. Discussion and conclusion

According to the review, all of the models need the experimental data to be calibrated in order to model the grounding electrode. The CIGRE, Bellaschi, and Liew-Darveniza models are dependent on the critical electric field value, whereas the Nor model needs the voltage and current waveforms. It should be noted that critical electric field value and the voltage and current data are mainly used to determine the minimum resistance value of the grounding electrode. Without these data, none of the models can model the grounding electrode accurately. All models can determine approximately the minimum grounding electrode resistance value relative to the current peak value. The error by the models in computing the grounding electrode resistance for the duration while current is in decay time is larger than the error of the values computed for the duration while current is in rise time. The CIGRE and Bellaschi models, in term of simplicity in computation, have advantages over the Nor and Liew-Darveniza models. The voltage peak values obtained by the CIGRE model are more accurate

compared to the voltage peak values obtained by the Nor and Liew-Darveniza models, as well as compared to the experimental values. Nor model can accurately simulate the voltage waveforms obtained by the experiment. However, Nor's model cannot be used to obtain the voltage waveform without experimental data. Liew-Darveniza's model is more accurate in terms of modelling the characteristics of the grounding electrode resistance due to the consideration of the energy balance concept. In addition, among the models, only Liew-Darveniza's model can represent the hysteresis characteristic of the grounding electrode resistance.

Acknowledgement

The authors wish to thank the Ministry of Science, Technology and Innovation (MOSTI), Ministry of Education (MOE), and Universiti Teknologi Malaysia (Research Vote Nos. 4S045, 03H59, and 4F291) for the financial aid.

References

- [1] Mokhtari M., Abdul-Malek Z., Salam Z., *The effect of soil ionization on transient grounding electrode resistance in non-homogeneous soil conditions*, International Transactions on Electrical Energy Systems 26: 1462-1475 (2016).
- [2] Mokhtari M., Abdul-Malek Z., *Progress Earthing Studies for Modern Life Style*, Universiti Teknologi Malaysia (2015).
- [3] Bellaschi P.L., Armington R.E., Snowden A.E., *Impulse and 60-cycle characteristics of driven grounds-II*, Transactions of the American Institute of Electrical Engineers 61(6): 349-363 (1942).
- [4] CIGRE Working Group 33-01 (Lightning) of Study Committee 33, *Overvoltages and insulation coordination, Guide to procedures for estimating the lightning performance of transmission lines*, Paris October (1991).
- [5] Mousa A.M., *The soil ionization gradient associated with discharge of high currents into concentrated electrodes*, IEEE Transactions on Power Delivery 9(3): 1669-1677 (1994).
- [6] Schon J.H., *Physical Properties of Rocks: Fundamentals and Principles of Petrophysics*, Elsevier (1998).
- [7] Snowden D.P., Erler J.W., *Initiation of electrical breakdown of soil by water vaporization*, IEEE Transactions on Nuclear Science 30(6): 4568-4571 (1983).
- [8] Van Lint V.A.J., Erler J.W., *Electric breakdown of earth in coaxial geometry*, IEEE Transactions on Nuclear Science 29(6): 1891-1896 (1982).
- [9] Leadon R.E., Flanagan T.M., Mallon C.E., Denson R., *Effect of ambient gas on arc initiation characteristics in soil*, IEEE Transactions on Nuclear Science 30(6): 4572-6 (1983).
- [10] Flanagan T.M., Mallon C.E., Denson R., Smith I., *Electrical breakdown characteristics of soil*, IEEE Transactions on Nuclear Science 29(6): 1887-1890 (1982).
- [11] Flanagan T.M., Mallon C.E., Denson R., Leadon R.E., *Electrical breakdown properties of soil*, IEEE Transactions on Nuclear Science 28(6): 4432-4439 (1981).
- [12] Nor N.M., Haddad A., Griffiths H., *Characterization of ionization phenomena in soils under fast impulses*, IEEE Transactions on Power Delivery 21(1): 353-361 (2006).
- [13] Liew A.C., Darveniza M., *Dynamic model of impulse characteristics of concentrated earths*, Proceedings of the Institution of Electrical Engineers 121(2): 123-135 (1974).
- [14] Manna T.K., Chowdhuri P., *Generalised equation of soil critical electric field E_C based on impulse tests and measured soil electrical parameters*, IET Generation Transmission Distribution 1(5): 811-817 (2007).
- [15] Kosztaluk R., Loboda M., Mukhedkar D., *Experimental study of transient ground impedances*, IEEE Power Engineering Review 1(11): 44-51 (1981).

- [16] *Handbook for improving overhead transmission line lightning performance*, Electrical Power Research Institution (EPRI) (2004).
- [17] Mokhtari M., Abdul-Malek Z., *The effect of grounding electrode parameters on soil ionization and transient grounding resistance using electromagnetic field approach*, Applied Mechanics and Materials 554: 628-32 (2014).
- [18] Dwight H.B., *Calculation of resistances to ground*, Electrical Engineering 55(12): 1319-1328 (1936).
- [19] Wang J., Liew A.C., Darveniza M., *Extension of dynamic model of impulse behavior of concentrated grounds at high currents*, IEEE Transactions on Power Delivery 20(3): 2160-2165 (2005).
- [20] Sekioka S., Lorentzou M.I., Philippakou M.P., Prousalidis J.M., *Current-dependent grounding resistance model based on energy balance of soil ionization*, IEEE Transactions on Power Delivery 21(1): 194-201 (2006).
- [21] Mokhtari M., Abdul-Malek Z., Salam Z., *An improved circuit-based model of a grounding electrode by considering the current rate of rise and soil ionization factors*, IEEE Transactions on Power Delivery 30(1): 211-219 (2015).